Thermal transport by phonons and electrons in aluminum, silver, and gold from first principles

Ankit Jain and Alan J. H. McGaughey[*]

Department of Mechanical Engineering, Carnegie Mellon University, Pittsburgh, Pennsylvania 15213, USA
(Received 30 November 2015; revised manuscript received 30 January 2016; published 19 February 2016)

Mode-dependent phonon and electron transport properties in Al, Ag, and Au are predicted using density functional theory and lattice dynamics calculations. The predicted thermal conductivities, electrical conductivities, electron-phonon coupling coefficients, and electron-phonon mass enhancement parameters are in agreement with experimental measurements. At a temperature of 100 K, the phonon contribution to the total thermal conductivity of Al is 5% in bulk and increases to 15% for a 50 nm thick film. In all three metals, phonons with mean free paths between 1 and 10 nm are the dominate contributors to the thermal conductivity at a temperature of 300 K, while the relevant electron mean free paths are 10–100 nm. Despite similar atomic masses, the phonon thermal conductivity of Al is an order of magnitude smaller than that of silicon due to a larger three-phonon phase space and stronger anharmonicity. These results will impact the interpretation of thermoreflectance experiments that can resolve carrier-level contributions to thermal conductivity.

There have been significant advances in the prediction of phonon properties and thermal conductivity in semiconductors from first principles [1–5]. Phonon transport in metals is mostly untouched, however, because of the small contribution of phonons to bulk thermal conductivity [6,7] and the computational complexity of rigorously modeling electron-phonon (e-p) interactions. Even though electrons dominate thermal and electrical transport in metals, phonons play a critical role in that the electron transport is limited by e-p scattering at intermediate and high temperatures (i.e., above one-tenth of the Debye temperature) [6,8]. Furthermore, e-p interactions are important in superconductivity [9], hot-carrier mobility [10,11], the response of a material abruptly heated by ion bombardment or laser irradiation [12,13], and thermal transport across metal-dielectric interfaces in thermoelectric [14,15] and plasmonic [16] devices. Separating and quantifying the phonon contribution to thermal conductivity in metals is needed to model electron-phonon nonequilibrium using a two-temperature model, for example, in the analysis of thermoreflectance experiments that can resolve carrier-level contributions to thermal conductivity [9,17–21].

Our objective is to predict the mode-dependent phonon transport properties and thermal conductivity of the non-magnetic face-centered-cubic metals aluminum (Al), silver (Ag), and gold (Au) from first principles by considering phonon-phonon (p-p) and e-p interactions. We will also predict mode-dependent electron transport properties and from these, the electron thermal and electrical conductivities. Electron-impurity and electron-electron interactions are not important at the temperatures of interest (100–500 K; the Debye temperatures of Al, Ag, and Au are 428, 225, and 165 K) and are not considered. Mode-dependent properties are essential for understanding the origin of macroscopically observable properties and for predicting the behavior of nanostructured materials. The predictions are made from first principles using density functional theory (DFT), density functional perturbation theory (DFPT), and lattice dynamics

calculations in conjunction with the Boltzmann transport equation (BTE) [22].

Tang *et al.* predicted mode-dependent phonon linewidths (i.e., the inverse of the phonon lifetimes) in Ag and Au from first principles, but only considered p-p interactions [23]. The electron thermal and electrical conductivities of Al and Au have been predicted from first principles [24–26], but only using the lowest-order variational solution of the BTE. This approach predicts lower bounds of these two properties and does not provide mode-dependent transport properties [27]. Using this variational solution, Bauer *et al.* found agreement between the predicted and experimental values for Al [26]. For Au, they underpredicted the experimental electron thermal conductivity and electrical conductivity by 15% at a temperature of 200 K. To our knowledge, the total and mode-dependent phonon thermal conductivities (including both p-p and e-p scattering) and mode-dependent electron thermal and electrical conductivities have yet to be reported.

By solving the BTE and using the Fourier law, the elements of the 3×3 phonon thermal conductivity tensor $\underline{k_p}$ are [28]

$$k_{p,\alpha\beta} = \frac{1}{V} \sum_{\boldsymbol{q}\nu} \hbar\omega_{\boldsymbol{q}\nu} \frac{\partial n_{\boldsymbol{q}\nu}}{\partial T} v_{\boldsymbol{q}\nu,\alpha} v_{\boldsymbol{q}\nu,\beta} \tau_{\boldsymbol{q}\nu}. \qquad (1)$$

The summation is over all the phonon modes in the first Brillouin zone enumerated by wave vector $\boldsymbol{q}$ and polarization ν. V is the crystal volume, $\hbar$ is the reduced Planck constant, $\omega_{\boldsymbol{q}\nu}$ is the phonon frequency, $n_{\boldsymbol{q}\nu}$ is the Bose-Einstein distribution, T is temperature, $v_{\boldsymbol{q}\nu,\alpha}$ is the α component of the phonon group velocity vector $\boldsymbol{v_{q\nu}}$, and $\tau_{\boldsymbol{q}\nu}$ is the phonon lifetime. Similar expressions for the electron thermal and electrical conductivities can be obtained from the BTE and the Onsager relations (see Sec. S1 in the Supplemental Material (SM) [29]).

We applied DFT and DFPT to calculate mode-dependent phonon and electron properties by considering p-p and e-p interactions under the relaxation time approximation (RTA) of the BTE. The e-p coupling coefficients were calculated using DFPT as implemented in QUANTUM ESPRESSO (QE) [22]. They were initially obtained on coarse 18×18×18 (electron) and 6×6×6 (phonon) wave vector grids and then interpolated to finer 80×80×80 (electron) and 32×32×32 (phonon) wave

*mcgaughey@cmu.edu
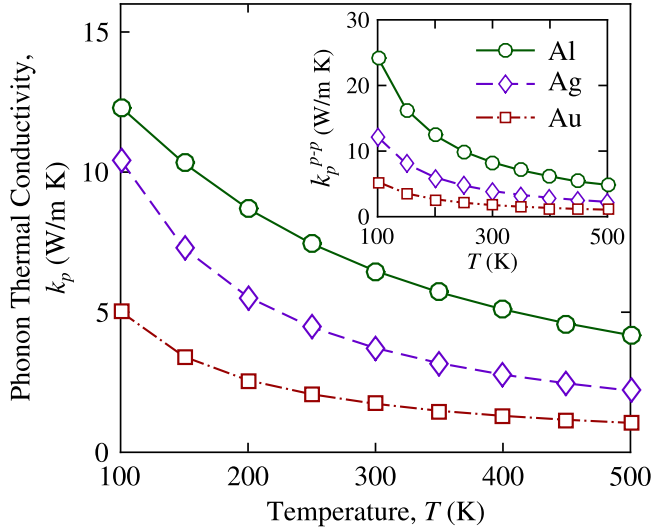
FIG. 1. Variation of phonon thermal conductivity k_p and (inset) phonon thermal conductivity obtained by considering only p-p scattering, $k_p^{p\text{-}p}$, with temperature for Al, Ag, and Au.

vector grids using the maximally localized Wannier functions basis as implemented in the electron-phonon Wannier (EPW) package [30]. The harmonic and cubic force constants required for the three-phonon scattering rate calculations were obtained using finite differencing of DFT forces. We calculated forces on 216 atom supercells with a $3\times3\times3$ electronic wave vector grid and the recommended plane wave energy cutoffs (Table S1) using the DFT package VASP [31]. The local density approximation exchange correlation was employed for all calculations. Further details about the calculations and their convergence are provided in Sec. S2.

We first plot the phonon thermal conductivities of Al, Ag, and Au obtained by considering (i) both p-p and e-p interactions (k_p) and (ii) only p-p interactions ($k_p^{p\text{-}p}$) in Fig. 1 and its inset for temperatures between 100 and 500 K [32]. For both k_p and $k_p^{p\text{-}p}$ at all temperatures, Al has the highest thermal conductivity, followed by Ag and Au. This trend is opposite to that of the atomic masses, with Al the lightest, followed by Ag and Au. Lower atomic mass results in higher phonon group velocities, which explains the relative values of the thermal conductivities. The decreasing thermal conductivity for all three metals with increasing temperature is typical of that of semiconductors. This trend is a result of increasing phonon populations with increasing temperature that lead to more scattering.

The effect of e-p interactions on the phonon thermal conductivity is strongest for Al. Upon addition of the e-p

interactions, its phonon thermal conductivity decreases by 50% at a temperature of 100 K, while the decrease is less for Ag (14%) and Au (6%). As will be shown later, this larger decrease in Al is due to stronger e-p coupling. With increasing temperature, p-p scattering becomes stronger due to an increase in the number of phonons. As a result, the effect of e-p scattering on the phonon thermal conductivity decreases with increasing temperature. These results point to the importance of considering both e-p and p-p scattering, particularly at lower temperatures.

Our predicted values of k_p, electron thermal conductivity (k_e), total thermal conductivity ($k = k_e + k_p$), and electrical conductivity (σ), at a temperature of 300 K are provided in Table I along with experimental measurements [6]. The variations of k_e and σ with temperature for all three metals are plotted in Fig. S7. All of our predictions are converged to within 11% with respect to the calculation parameters (Sec. S3). This convergence threshold is comparable to the agreement between first-principles-predicted and experimentally measured thermal conductivities of semiconductors [4,39]. For k, our predictions are within 13% of the measurements. For σ, our predictions agree within 6% of the measurements for Al and Ag. For Au, there is a 25% underprediction, which is consistent with the DFT calculations of Bauer *et al.* [26]. We believe that this underprediction is due to (i) sensitivity of the Fermi surface to the lattice constant [26] (see Table S1 for the predicted lattice constants), (ii) the resolution of the electronic wave vector grid (see Fig. S5 for the variation of k_e and σ with the electronic wave vector grid for Au), and/or (iii) use of the RTA solution of the BTE.

We next plot the k_p and k_e accumulation functions of Al, Ag, and Au at a temperature of 300 K with respect to the carrier mean free path (MFP) in Figs. 2(a) and 2(b). The MFP, Λ, is a measure of the distance traveled by a carrier between scattering events and is the product of the magnitude of its velocity and its lifetime (e.g., for phonon mode $q\nu$, $\Lambda_{q\nu} = |\mathbf{v}_{q\nu}|\tau_{q\nu}$). The accumulation function describes the contribution of carriers of different MFPs to thermal conductivity. The central 90% of k_p comes from phonons with MFPs between 2 and 62 nm in Ag and between 1 and 64 nm in Au. In Al, the k_p accumulation is steep, with the central 90% coming from phonons with MFPs that span only one order of magnitude (2–22 nm).

In contrast to the k_p accumulations, which start around a phonon MFP of 1 nm, the electron MFPs that contribute to k_e start at 10 nm for Al and 20 nm for Ag and Au. Furthermore, the range of MFPs that contribute to k_e is much smaller than that of the phonon systems, spanning a factor of 2. The central 90% of k_e comes from electrons with MFPs between 10 and 25, 32 and 56, and 22 and 41 nm for Al, Ag, and Au. This narrow

TABLE I. Phonon thermal conductivity (k_p), electron thermal conductivity (k_e), total thermal conductivity (k), electrical conductivity (σ), e-p coupling factor (G), and e-p mass enhancement parameter (λ) for Al, Ag, and Au at a temperature of 300 K. For G, the electron and phonon temperatures are 400 and 300 K [Eq. (2)]. The numbers in parentheses are experimental measurements/textbook values. The σ data from Ref. [6] are at a temperature of 295 K.

Metal	k_p (W/m K)	k_e (W/m K)	k (W/m K)	σ (10^7 S/m)	G (10^{16} W/m^3 K)	λ
Al	6	246	252 (237 [6])	3.46 (3.65 [6])	53.8 (24.5 [33])	0.49 (0.38–0.48 [8])
Ag	4	370	374 (429 [6])	5.89 (6.21 [6])	3.0 (3.5 [34])	0.16 (0.09–0.17 [8])
Au	2	276	278 (317 [6])	3.42 (4.55 [6])	2.2 (2.2–3.5 [33,35–38])	0.18 (0.12–0.22 [8])
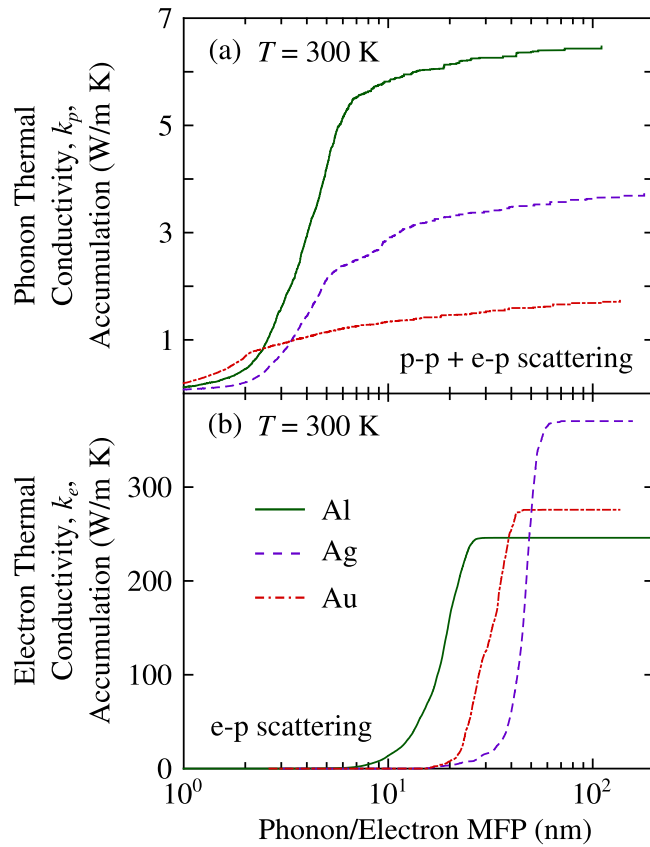
FIG. 2. (a) Phonon (k_p) and (b) electron (k_e) thermal conductivity accumulation functions with respect to phonon/electron MFP for Al, Ag, and Au at a temperature of 300 K.

range of electron MFPs corroborates the suitability of the gray approximation for electron transport in metals (i.e., the use of a single MFP), which is known to be a poor approximation for phonons in most semiconductors [40].

Phonon MFPs in semiconductors are typically one to three orders of magnitude larger than the electron MFPs [41]. As can be seen from Figs. 2(a) and 2(b), however, the phonon MFPs in Ag, Al, and Au are an order of magnitude smaller than the electron MFPs. This separation of length scales becomes important in nanostructured materials (e.g., thin films, nanowires, nanocrystalline materials), where bulk MFPs are reduced due to boundary scattering. At a temperature of 100 K, the contribution of phonons towards the total bulk thermal conductivity is 5% (Al), 2% (Ag), and 2% (Au). In a 50 nm thick film, as would be present as the transducer in a thermoreflectance experiment [19], the phonon contribution to the cross-plane thermal conductivity increases to an appreciable 15% (Al), 13% (Ag), and 9% (Au) (calculation details in Sec. S7).

To determine the origin of the small phonon MFPs in metals, we next compare phonon transport in Al with the well-studied semiconductor silicon (Si) by considering only p-p interactions (see Sec. S8 for details on the Si calculations). Al and Si have similar atomic masses (27 and 28 Da for isotopically enriched specimens) and sit next to each other on the periodic table. As can be seen from the k_p^{p-p} accumulation functions plotted in Fig. 3(a), however, the phonon MFPs in Si
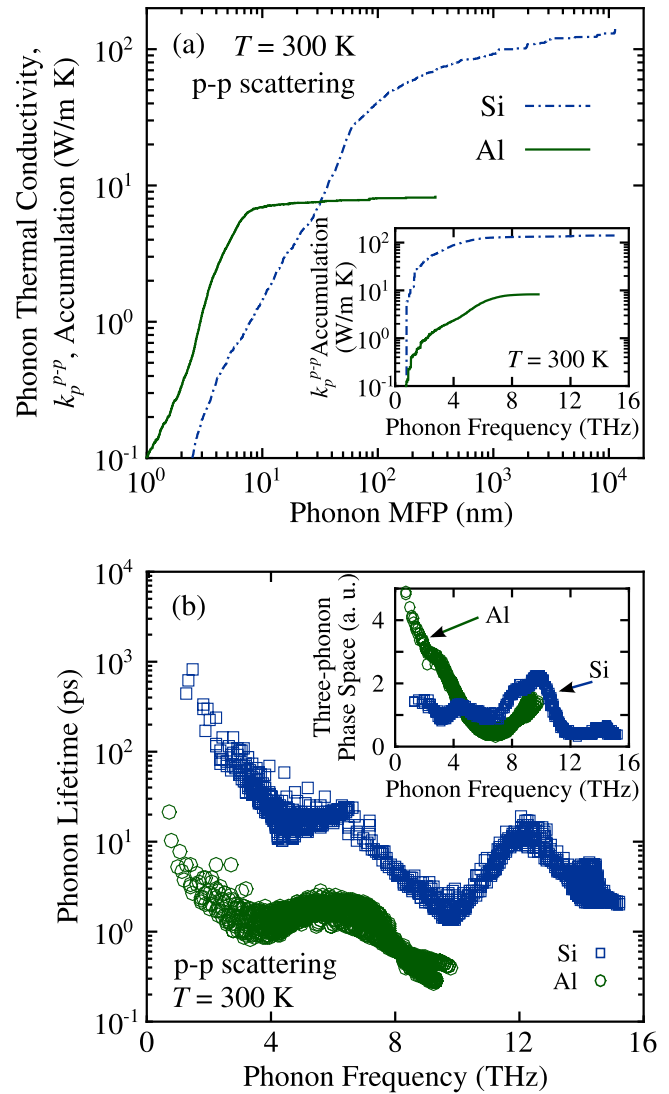
FIG. 3. For Al and Si at a temperature of 300 K, only considering p-p scattering: (a) Phonon thermal conductivity accumulation with respect to MFP. The inset shows the accumulation with respect to frequency. (b) Variation of phonon lifetimes with frequency. The inset shows the frequency dependence of the three-phonon phase space.

span four orders of magnitude ($2\,\mathrm{nm}-10\,\mu\mathrm{m}$) as compared to less than an order of magnitude in Al ($1-8\,\mathrm{nm}$) at a temperature of 300 K. Consequently, the predicted k_p^{p-p} of Si and Al at this temperature using the RTA solution of BTE are 140 and 8 W/m K. The phonon group velocities in Al are smaller than those in Si due its lower mass density and weaker metallic bonds, as is evident from the maximum phonon vibration frequency of 9 THz in Al as opposed to 15 THz in Si, as shown in Fig. S9(a). The differences in the group velocities, however, cannot fully explain the orders of magnitude difference in the MFPs. To further isolate this difference, we plot the phonon lifetimes for Al and Si at a temperature of 300 K in Fig. 3(b).

Phonons with frequencies of less than 5 THz have up to two orders of magnitude larger lifetimes in Si than in Al. For phonons with frequencies larger than 5 THz, the Si lifetimes are one order of magnitude larger. As a result, as can be seen from the inset of Fig. 3(a), at a temperature of 300 K, phonons

with frequencies less than 5 THz contribute 108 W/m K (76%) to the thermal conductivity of Si while their contribution is less than 4 W/m K (44%) in Al (for $k_p^{p\text{-}p}$). This difference in the phonon lifetimes in Al and Si can be understood by comparing their three-phonon phase spaces and anharmonicities.

The three-phonon phase space is calculated by counting the number of p-p processes that satisfy the phonon energy and momentum conservation selection rules [42]. It is thus a harmonic-level property of a material. As can be seen from the inset plot of Fig. 3(b), for phonons with frequencies less than 5 THz, the three-phonon phase space in Al is up to five times larger than that in Si. The greater number of possible p-p scattering events leads to lower lifetimes.

To quantify the phonon anharmonicity, we calculated mode-dependent Grüneisen parameters, which are plotted in Fig. S9(b). Larger Grüneisen parameters correspond to stronger anharmonicity. For Si, all values are less than 2, whereas for Al they are as high as 5. The heat-capacity-weighted mode-averaged Grüneisen parameter is 2.2 in Al as opposed to 1.0 in Si at a temperature of 300 K (Sec. S9), indicating stronger anharmonicity and thus increased phonon-phonon scattering and lower lifetimes.

We next focus our attention on the e-p coupling factor G, which is an input to two-temperature models. It was defined by Anisimov *et al.* [12] and Allen [9] to study the relaxation of hot electrons as

$$G = \frac{1}{(T_e - T_p)} \frac{\partial E^{e\text{-}p}}{\partial t}, \qquad (2)$$

where $\frac{\partial E^{e\text{-}p}}{\partial t}$ is the energy transfer rate between hot electrons at a temperature T_e and phonons (i.e., the lattice) at a temperature T_p [see Eq. (S22) for the $\frac{\partial E^{e\text{-}p}}{\partial t}$ calculation details].

Our predicted values of G for $T_e = 400$ K and $T_p = 300$ K are reported in Table I, along with results extracted from experiments. G is highest for Al, followed by Ag and Au, consistent with the results shown in Fig. 1. Our prediction of G for Au falls at the lower end of the wide range of experimental values [33,35–38], which span a factor of almost 2. Only one experimental value is available for each of Al and Ag. For Al, our prediction is double that of the experiment (which was extrapolated from film-thickness- and grain-size-dependent data [33]), while for Ag, our prediction is 20% higher.

To see the effect of laser heating intensity (related to T_e) and T_p on G, which are both relevant in thermoreflectance experiments, we plot the dependence of G on T_e and T_p in Figs. S10 and S11. For all three metals, the change in G is (i) less than 7% in varying T_e from 400 to 800 K at $T_p = 300$ K and (ii) less than 14% in varying T_p from 100 to 300 K at $T_e = 400$ K.

We plot the contribution of different phonon modes towards G at $T_p = 300$ K and $T_e = 400$ K in the inset of Fig. S10 for all three metals. In Al, 90% of the contribution towards G comes from phonons with frequencies larger than 4.9 THz, while it is from phonons with frequencies larger than 2.3 and 1.8 THz in Ag and Au. These different frequency ranges will affect what phonon modes are excited at the interface between a thin metal transducer and a dielectric substrate. This information is critical for interpreting thermoreflectance experiments [18,19,21].

We also report the e-p mass enhancement parameter λ in Table I [Eq. (S23)], which is another measure of the e-p interaction strength and can be used to calculate G under the assumption of an electron-state-independent e-p coupling matrix element [$g_{mn}^{\nu}(\boldsymbol{k}\boldsymbol{k}',\boldsymbol{q})$ in Eq. (S22)] [9,13,43]. As opposed to G, which is a nonequilibrium property, λ is an equilibrium property that can be extracted from measurements of heat capacity, Fermi velocity, and critical superconductivity temperature [8]. Our predicted values of λ are within reported ranges [8] and follow the same trend as the G values, giving confidence to our first-principles framework.

In summary, we used first-principles calculations to study mode- and temperature-dependent phonon and electron transport properties in Al, Ag, and Au by considering both e-p and p-p scattering. Good agreement was found with experimental measurements and the calculation framework can be directly extended to all nonmagnetic metals. The results elucidate the origin of small intrinsic phonon MFPs in metals and the important contributions of phonons to thermal transport in thin metal films. The ability to calculate mode-dependent phonon and electron properties will enable the design of other metallic nanostructures with tailored thermal conductivity. Our findings are particularly relevant to the interpretation of thermoreflectance experiments for measuring thermal conductivity accumulation functions, where phonon-electron nonequilibrium at a metal-semiconductor interface plays a critical role.

---

[1] D. A. Broido, M. Maloney, G. Birner, N. Mingo, and D. Stewart, Appl. Phys. Lett. **91**, 231922 (2007).

[2] K. Esfarjani, G. Chen, and H. T. Stokes, Phys. Rev. B **84**, 085204 (2011).

[3] J. Garg, N. Bonini, B. Kozinsky, and N. Marzari, Phys. Rev. Lett. **106**, 045901 (2011).

[4] L. Lindsay, D. A. Broido, and T. L. Reinecke, Phys. Rev. B **87**, 165201 (2013).

[5] B. Liao, B. Qiu, J. Zhou, S. Huberman, K. Esfarjani, and G. Chen, Phys. Rev. Lett. **114**, 115901 (2015).

[6] C. Kittel, *Introduction to Solid State Physics*, 6th ed. (Wiley, New York, 1986).

[7] J. M. Ziman, *Electrons and Phonons* (Oxford University Press/ Clarendon, Oxford, UK, 1960).

[8] G. Grimvall, *The Electron-Phonon Interaction in Metals*, (North-Holland, Amsterdam, 1981), Vol. 8.

[9] P. B. Allen, Phys. Rev. Lett. **59**, 1460 (1987).

[10] C. Herring, Phys. Rev. **96**, 1163 (1954).

[11] M. Bernardi, J. Mustafa, J. B. Neaton, and S. G. Louie, Nat. Commun. **6**, 7044 (2015)

[12] S. I. Anisimov, B. L. Kapeliovich, and T. L. Perelman, Zh. Eksp. Teor. Fiz. **66**, 776 (1974) [Sov. Phys. JETP **39**, 375 (1974)].

[13] Z. Lin, L. V. Zhigilei, and V. Celli, Phys. Rev. B **77**, 075133 (2008).

[14] R. Venkatasubramanian, E. Siivola, T. Colpitts, and B. O'quinn, Nature (London) **413**, 597 (2001).

[15] L. Zhang, J.-T. Lü, J.-S. Wang, and B. Li, J. Phys.: Condens. Matter **25**, 445801 (2013).

[16] A. Principi, M. Carrega, M. B. Lundeberg, A. Woessner, F. H. L. Koppens, G. Vignale, and M. Polini, Phys. Rev. B **90**, 165408 (2014).

[17] M. I. Kaganov, I. M. Lifshitz, and L. V. Tanatarov, Zh. Eksp. Teor. Fiz. **31**, 232 (1957) [Sov. Phys. JETP **4**, 173 (1957)].

[18] A. J. Minnich, J. A. Johnson, A. J. Schmidt, K. Esfarjani, M. S. Dresselhaus, K. A. Nelson, and G. Chen, Phys. Rev. Lett. **107**, 095901 (2011).

[19] K. T. Regner, D. P. Sellan, Z. Su, C. H. Amon, A. J. McGaughey, and J. A. Malen, Nat. Commun. **4**, 1640 (2013).

[20] R. B. Wilson, J. P. Feser, G. T. Hohensee, and D. G. Cahill, Phys. Rev. B **88**, 144305 (2013).

[21] K. T. Regner, J. P. Freedman, and J. A. Malen, Nanoscale Microscale Thermophys. Eng. **19**, 183 (2015).

[22] P. Giannozzi, S. Baroni, N. Bonini, M. Calandra, R. Car, C. Cavazzoni, D. Ceresoli, G. L. Chiarotti, M. Cococcioni, I. Dabo, A. D. Corso, S. de Gironcoli, S. Fabris, G. Fratesi, R. Gebauer, U. Gerstmann, C. Gougoussis, A. Kokalj, M. Lazzeri, L. Martin-Samos, N. Marzari, F. Mauri, R. Mazzarello, S. Paolini, A. Pasquarello, L. Paulatto, C. Sbraccia, S. Scandolo, G. Sclauzero, A. P. Seitsonen, A. Smogunov, P. Umari, and R. M. Wentzcovitch, J. Phys.: Condens. Matter **21**, 395502 (2009).

[23] X. Tang and B. Fultz, Phys. Rev. B **84**, 054303 (2011).

[24] S. Y. Savrasov and D. Y. Savrasov, Phys. Rev. B **54**, 16487 (1996).

[25] E. G. Maksimov, D. Y. Savrasov, and S. Y. Savrasov, Phys. Usp. **40**, 337 (1997).

[26] R. Bauer, A. Schmid, P. Pavone, and D. Strauch, Phys. Rev. B **57**, 11276 (1998).

[27] P. B. Allen, Phys. Rev. B **17**, 3725 (1978).

[28] G. D. Mahan, *Many-Particle Physics* (Springer, Berlin, 2013).

[29] See Supplemental Material at http://link.aps.org/supplemental/ 10.1103/PhysRevB.93.081206 for details on the computational methodology, convergence testing, electron and phonon heat capacities, temperature-dependent electrical and electron thermal conductivities, thin film thermal conductivities, silicon calculations, and electron-phonon coupling parameter.

[30] F. Giustino, M. L. Cohen, and S. G. Louie, Phys. Rev. B **76**, 165108 (2007).

[31] The relaxed lattice constants obtained from QE and VASP are within 0.5% of each other for all three metals. We used the QE relaxed lattice constants for the force calculations from VASP. See Sec. S2 for more details.

[32] The p-p scattering rates are obtained using the RTA solution of the BTE. We found the difference between $k_p^{p\text{-}p}$ predicted from the RTA and a full solution of BTE [44] to be 27% (Al), 16% (Ag), and 10% (Au) at a temperature of 300 K.

[33] J. L. Hostetler, A. N. Smith, D. M. Czajkowsky, and P. M. Norris, Appl. Opt. **38**, 3614 (1999).

[34] R. H. M. Groeneveld, R. Sprik, and A. Lagendijk, Phys. Rev. Lett. **64**, 784 (1990).

[35] R. W. Schoenlein, W. Z. Lin, J. G. Fujimoto, and G. L. Eesley, Phys. Rev. Lett. **58**, 1680 (1987).

[36] R. H. M. Groeneveld, R. Sprik, and A. Lagendijk, Phys. Rev. B **51**, 11433 (1995).

[37] J. Hohlfeld, S.-S. Wellershoff, J. Güdde, U. Conrad, V. Jähnke, and E. Matthias, Chem. Phys. **251**, 237 (2000).

[38] W. Wang and D. G. Cahill, Phys. Rev. Lett. **109**, 175503 (2012).

[39] A. Jain and A. J. McGaughey, Comput. Mater. Sci. **110**, 115 (2015).

[40] C. Dames and G. Chen, in *Thermoelectrics Handbook: Macro to Nano*, edited by D. M. Rowe (CRC Press, Boca Raton, FL, 2005), Chap. 42, pp. 42-1–42-11.

[41] A. I. Hochbaum, R. Chen, R. D. Delgado, W. Liang, E. C. Garnett, M. Najarian, A. Majumdar, and P. Yang, Nature (London) **451**, 163 (2008).

[42] L. Lindsay and D. A. Broido, J. Phys.: Condens. Matter **20**, 165209 (2008).

[43] X. Y. Wang, D. M. Riffe, Y.-S. Lee, and M. C. Downer, Phys. Rev. B **50**, 8016 (1994).

[44] L. Lindsay, D. A. Broido, and N. Mingo, Phys. Rev. B **82**, 115427 (2010).